Smart Structures and Systems, *Vol. 30, No. 2 (2022) 121-133*
https://doi.org/10.12989/sss.2022.30.2.121

Free vibration analysis of a sandwich cylindrical shell with an FG core based on the CUF

Kamran Foroutan [1a], Habib Ahmadi*[1] and Erasmo Carrera [2b]

[1] *Faculty of Mechanical Engineering, Shahrood University of Technology, Shahrood, Iran*
[2] *Mul[2] Group, Department of Mechanical and Aerospace Engineering, Politecnico di Torino, Turin, Italy*

(*Received October 9, 2020, Revised December 12, 2020, Accepted April 19, 2022*)

Abstract. An analytical approach for the free vibration behavior of a sandwich cylindrical shell with a functionally graded (FG) core is presented. It is considered that the FG distribution is in the direction of thickness. The material properties are temperature-dependent. The sandwich cylindrical shell with a FG core is considered with two cases. In the first model, i.e., Ceramic-FGM-Metal (CFM), the interior layer of the cylindrical shell is rich metal while the exterior layer is rich ceramic and the FG material is located between two layers and for the second model i.e., Metal-FGM-Ceramic (MFC), the material distribution is in reverse order. This study develops Carrera's Unified Formulation (CUF) to analyze sandwich cylindrical shell with an FG core for the first time. Considering the Principle of Virtual Displacements (PVDs) according to the CUF, the dependent boundary conditions and governing equations are obtained. The coupled governing equations are derived using Galerkin's method. In order to validate the present results, comparisons are made with the available solutions in the previous researches. The effects of different geometrical and material parameters on the free vibration behavior of a sandwich cylindrical shell with an FG core are examined.

Keywords: Carrera's unified formulation; free vibration analysis; functionally graded material; principle of virtual displacements; sandwich cylindrical shell

1. Introduction

Recently, FG structures reinforced by stiffeners are widely utilized in different industry branches. Also, the application of sandwich structures in various fields of engineering, including aerospace, mechanical, and civil, has been widely developed in recent years. According to their low weight and high performance, the attention of engineers and researchers were attracted to study their structural behavior. This kind of structure exhibits several advantages such as, high strength to low weight ratio, good thermal isolation, improved nonlinear capacity, decent local and global buckling behavior and so on. Moreover, the application of composite materials in many commercial aircraft indicates the importance of studying these types of structures in both aerospace and aeronautical industries (Gohardani *et al*. 2014). FG sandwich has a favorable mechanical property in the special high-temperature environments due to the core fabrication with FG material with a continuous variation of the material properties along a specific direction and the high stiffness to weight ratio of the design of the sandwich structures. Thus, the FG sandwich structures have been widely applied in the actual industrial application as fundamental ones of the system, such as bridges, architectural structures, hydraulic structures, and so on. Some studies have been focused on the nonlinear analyses of functionally graded (FG) and composite structures. The vibration response of cylindrical panels with the FG material via the theory of higher-order shear deformation shell was examined by Babaei *et al*. (2019). Sofiyev *et al*. (2017) studied the vibration behavior of the composite cylindrical shells resting on the elastic foundation via the shear deformation theory (SDT). Nonlinear vibrations of metal foam cylindrical shells reinforced with graphene platelets and FG sandwich thin nanoshells conveying fluid incorporating surface stress influence were analyzed by Wang *et al*. (2019a, b). The vibration response of a composite cylindrical shell was presented by Zhang *et al*. (2018). Free and forced vibrations of nanocomposite beams reinforced by 3D graphene foam were analyzed by Yang and Wang (2020). Giunta *et al*. (2013) investigated the vibration response of simply supported, cross-ply beams utilizing refined theories. Zhang *et al*. (2014) investigated the thermal buckling analysis of functionally graded plates using a local Kriging meshless method. The nonlinear thermomechanical analysis of moderately thick functionally graded plates using a local Petrov–Galerkin approach with moving Kriging interpolation was studied by Zhu *et al*. (2014). An element-free IMLS-Ritz method for the numerical solution of three-dimensional wave equations and an element-free computational framework for elastodynamic problems based on the IMLS-Ritz method was presented by (Zhang *et al*. 2015a, b). Vibration behaviors of FG porous plates with

*Corresponding author, Ph.D.,
E-mail: habibahmadif@shahroodut.ac.ir
[a] Ph.D., E-mail: kamran.foroutan@shahroodut.ac.ir
[b] Professor, E-mail: erasmo.carrera@polito.it

ISSN: 1738-1584 (Print), 1738-1991 (Online)

different loads were investigated by Wang (2018), Wang and Zu (2017a, b, c). Also, the Chebyshev collocation technique for vibration analysis of sandwich cylindrical shells with metal foam core and free vibration analysis of metal foam core sandwich beams on elastic foundation using Chebyshev collocation method was examined by Wang *et al*. (2020), Wang and Zhao (2019).

Some research is paid attention to vibration analyses of the stiffened cylindrical shell with the functionally graded material. Duc and Thang (2015) investigated the vibration analysis of the cylindrical shells reinforced by stiffeners with the FGM and initial imperfection resting on the elastic foundation exposed to the damping and mechanical loads. The vibration response of the cylindrical shell reinforced by stiffeners with the FGM embedded within an elastic foundation exposed to the external excitation was examined by Dung and Nam (2014). Foroutan *et al*. (2019b) addressed the vibration of spiral stiffened cylindrical shells embedded within an elastic foundation. Bich *et al*. (2013) presented the static and dynamic responses of stiffened cylindrical shells with functionally graded material. The vibration of spiral stiffened cylindrical shells with FGM embedded within the nonlinear elastic foundation exposed to the axial excitation was examined by Foroutan *et al*. (2018).

In the previous literature, the researchers have not investigated the vibration analyses of carbon nanotube (CNT) cylindrical shell and plate. Some researchers have been focused on the nonlinear behavior of the cylindrical shells and plates stiffened by a CNT.

The buckling and post-buckling analysis of FG-CNT plate with different methods have been investigated by Zhang (2017a), Zhang and Liew (2016a), Zhang *et al*. (2015c, 2016a, b, c). Predicting bucking and vibration behaviors of FG-CNT reinforced composite cylindrical panels with three-dimensional flexibilities were examined by Liew and Alibeigloo (2020). Liew *et al*. (2020) studied the recent progress of FG-CNT reinforced composites and structures. Pan *et al*. (2019) presented the modeling geometrically nonlinear large deformation behaviors of matrix cracked hybrid composite deep shells containing CNTRC layers. Also, nonlinear, free, and forced vibration behaviors of FG-CNT plate under various loads with different methods have been analyzed by Lei *et al*. (2015a), Zhang (2017b, c), Zhang and Liew (2015, 2016b), Zhang *et al*. (2015d, e, f, 2016d, e, f, g, h). Nonlinear analyses of FG-CNT cylindrical panels and shells subjected to the different loads have been studied by Lei *et al*. (2014), Zhang *et al*. (2017, 2016i). Nonlinear vibration of a micro cylindrical shell reinforced by carbon nanotubes (CNTs) with considering agglomeration effects was analyzed by Tohidi *et al*. (2018). Zghal *et al*. (2018) studied the free vibration behavior of FG composite shells reinforced by CNT utilizing the first-order shear deformation theory and Chebyshev-Ritz formulation. Nonlinear and vibration analyses of laminated FG-CNT plate with different methods have been investigated by Zhang and Xiao (2017), Zhang and Selim (2017), Lei *et al*. 2016, 2015b). Nonlinear vibration behavior of piezoelectric plates reinforced with CNT via the differential quadrature method was examined by Arani *et al*. (2016). Shen and Xiang (2012) reported the vibration of CNTRC skew cylindrical shells with FGM utilizing the formulation of Chebyshev-Ritz. The vibration of cylindrical shells stiffened by a CNT in thermal environments was investigated by Song *et al*. (2016). Foroutan *et al*. (2019a) addressed the vibration of imperfect FG cylindrical panels stiffened by a CNT under a thermal environment subjected to external pressure. The vibration responses of CNTRC cylindrical shells with the FGM under the thermal conditions were presented by Chakraborty *et al*. (2019). The vibration and stability responses of the cylindrical panels with FGM reinforced by a carbon nanotube via the semi-analytical approach investigated by Qin *et al*. (2019). Carrera and Ettore (1995) investigated the vibration of rotating CNTRC cylindrical shells with FGM and arbitrary boundary conditions.

A class of two-dimensional (2D) theories utilizing a compact notation was introduced by Carrera (1997), which in literature; was later named Carrera's Unified Formulation (CUF). The above-mentioned compact notation can be expanded the field of displacement to arbitrary expansion order. For this purpose, a single 3 × 3 matrix has been used, which is named as fundamental nuclei. These fundamental nuclei can be utilized to show the approaches of the variable description, such as Layer-wise (LW) and Equivalent Single Layer (ESL) models (Carrera 1998a, b, c, 2003, Carrera and Demasi 2002a, b). Carrera *et al*. (2011) has been investigated the theoretical foundations of the unified method. Recently, CUF has also been utilized in the formulation of the shell, plate, and beam theories (Pagani *et al*. 2013, Carrera and Pagani 2014, Carrera 1999, Cinefra *et al*. 2015a, b, c, Neves *et al*. 2012, Mashat *et al*. 2014, Viglietti *et al*. 2019).

Considering previous works, it is indicated that there is no research on the free vibration of a sandwich cylindrical shell with an FG core according to the CUF. Therefore, the novelties of the present paper may be summarized as follows:

(i) Development of the Carrera's Unified Formulation (CUF) for the free vibration behavior of a sandwich cylindrical shell with an FG core for the first time. The 3D displacement field $u(x, y, z)$ according to the CUF for the 2D plate theory, can be expanded as a set of thickness functions depending only on the thickness coordinate z and the corresponding variables depending on the in-plane coordinates x and y.
(ii) A sandwich cylindrical shell with an FG core has three layers, including the ceramic, FGM and metal in two cases, which is examined as a three-dimensional (3D) structure. Also, the material properties are temperature-dependent.
(iii) Furthermore, the resilience of the thickness, which is neglected in most of the researches on functionally graded structures, as well as continuity of the displacement field and the zig-zag form in layered structures, are investigated in this paper.

To this end, the governing equations based on the CUF

are obtained, and in order to validate the present results, comparisons are made with the available solutions in the previous researches. The effects of different geometrical and material parameters on the vibration of a sandwich cylindrical shell with an FG core are examined.

2. Sandwich cylindrical shell with FG core

The sandwich cylindrical shell with an FG core that the system of coordinate $(x,\ \theta,\ z)$ is illustrated in Fig. 1, in which the axes of x, θ and z are the axial, circumferential, and radial coordinate variables of the sandwich cylindrical shell with a FG core, respectively. The cylindrical shell has radius R, thickness h, and length L.

The volume fractions regarding the power-law are as (Ahmadi and Foroutan 2020)

$$V_c(z) = \left(\frac{2z+h}{2h}\right)^K \qquad V_m(z) = 1 - V_c(z) \tag{1}$$

In Eq. (1), $K \geq 0$ is the shell material power-law index. The subscripts m and c are referred to the metal and ceramic, respectively. A material coefficient P is defined as a temperature nonlinear function (Duc and Thang 2015, Foroutan *et al*. 2019a)

$$\mathrm{P} = \mathrm{P}_0(\mathrm{P}_{-1}T^{-1} + 1 + \mathrm{P}_1 T + \mathrm{P}_2 T^2 + \mathrm{P}_3 T^3) \tag{2}$$

In the present study, a sandwich cylindrical shell with an FG core is assumed in two cases which are shown in Fig. 2.

Considering the mentioned law, Young's modulus and mass density are obtained as (Nam *et al*. 2018, Wu and Li 2012, Arefi 2015):

Case I: Metal-FGM-Ceramic

$$[E(z),\rho(z)] = \begin{cases} (E_m,\rho_m) & t_0 \leq z \leq t_1 \\ (E_m,\rho_m) + (E_{cm},\rho_{cm})\left(\dfrac{2z+h_m}{2h_m}\right)^K & t_1 \leq z \leq t_2 \\ (E_c,\rho_c) & t_2 \leq z \leq t_3 \end{cases} \tag{3a}$$

Case II: Ceramic-FGM-Metal

$$[E(z),\rho(z)] = \begin{cases} (E_c,\rho_c) & t_0 \leq z \leq t_1 \\ (E_c,\rho_c) + (E_{mc},\rho_{mc})\left(\dfrac{2z+h_m}{2h_m}\right)^K & t_1 \leq z \leq t_2 \\ (E_m,\rho_m) & t_2 \leq z \leq t_3 \end{cases} \tag{3b}$$

where ρ, and E are the mass density and Young's modulus of the multilayer FG shell, respectively.

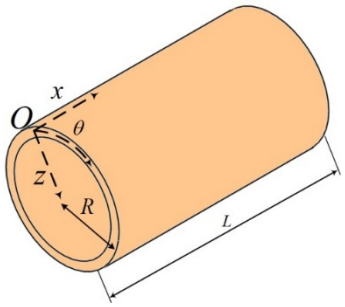

Fig. 1 Configuration of a sandwich cylindrical shell with an FG core

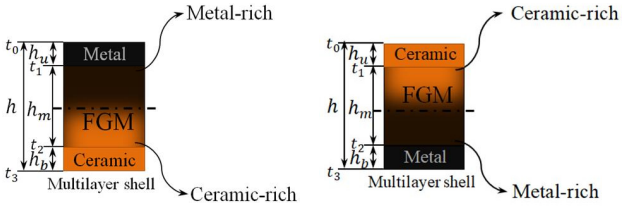

Case I: Metal-FGM-Ceramic Case II: Ceramic-FGM-Metal

Fig. 2 The material distribution of sandwich cylindrical shell with an FG core

3. Governing equation based on the CUF

3.1 Displacement base field

With regard to the CUF, three components of displacement are represented as a set of functions of thickness for the *k*th layer in a layered cylindrical shell and the respective displacement, which is related to the in-plane coordinates. According to above-mentioned expiations, displacement $\mathrm{u}^k(x,\theta,z) = \{u^k(x,\theta,z), v^k(x,\theta,z), w^k(x,\theta,z)\}^T$ can be written in the following expansion

$$\mathrm{u}^k(x,\theta,z) = F_\tau^k(z)\mathrm{u}_\tau^k(x,\theta) \qquad \delta\mathrm{u}^k(x,\theta,z) = F_s^k(z)\delta\mathrm{u}_s^k(x,\theta) \tag{4}$$

In Eq. (4), N is the expansion order utilized for the direction of thickness and $s,\tau = 0,1,\ldots,N$. Also, repetitious indexes are implicitly summed over considering the convention of Einstein summation. As shown in Fig. 3, subscripts $s,\tau = N$, and $s,\tau = 0$ show the values of the bottom and top surface, respectively. Also, other subscripts expressed the surfaces among the bottom and top surfaces.

The models of Equivalent Single Layer (ESL) are created, when one of the heterogeneous laminated structures treats as a statically equivalent single layer having a behavior of the complex constitutive. For $\frac{1}{1-z}$, the first few terms of the series of Maclaurin are utilized as functions of thickness to include by the other models of ESL.

$$F_0 = z^0 = 1,\ \ F_r = z^r,\ \ F_N = z^N \qquad r = 1,\ldots,N-1 \tag{5}$$

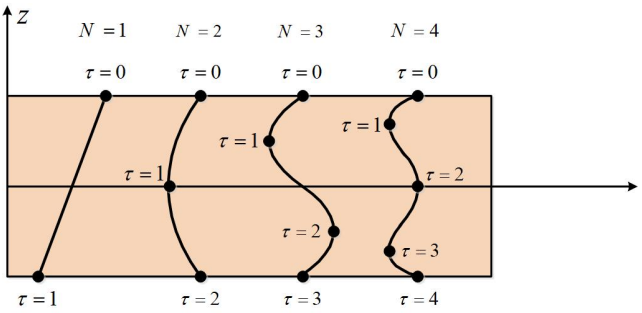

Fig. 3 Linear and higher-order distribution of displacements according to the CUF

and when the expansions for the direction of thickness are assumed separately for each layer of the multilayer, these models are Layer-Wise (LW). Therefore, to guarantee the continuation of the displacement at the interfaces among adjoining layers, the functions of thickness should have the properties which are in the following form

$$\begin{cases} F_0^k = 1, \ F_r^k = 0, \ F_N^k = 0 & \text{at top surface} \\ F_0^k = 0, \ F_r^k = 0, \ F_N^k = 1 & \text{at bottom surface} \end{cases} \tag{6}$$

As mentioned above, subscripts N and 0 are referred to the values of the bottom and top surface, respectively. r refers to the surfaces for among them. A Legendre polynomials mixture satisfies the above-mentioned properties. Considering that the Legendre polynomials are presented on the interlude $[-1,+1]$, ξ is utilized as the dimension of thickness.

$$\xi_k = \frac{2z}{z_{top}^k - z_{bot}^k} - \frac{z_{top}^k + z_{bot}^k}{z_{top}^k - z_{bot}^k} \tag{7}$$

In Eq. (7), z_{bot}^k and z_{top}^k are the coordinates of thickness for the bottom and top surface of the kth layer, respectively. Thickness functions to form the combination of Legendre polynomials are considered as

$$\begin{aligned} F_0^k &= \frac{P_0^k + P_1^k}{2}, \qquad F_N^k = \frac{P_0^k - P_1^k}{2} \\ F_r^k &= P_{r+1}^k - P_{r-1}^k \qquad r = 1, \dots, N-1 \end{aligned} \tag{8}$$

$P_1^k(\xi_k) = \xi_k$ and $P_0^k(\xi_k) = 1$ are the first two Legendre polynomials. Also, the higher-order Legendre polynomials are obtained recursively utilizing the equation in the following form

$$(n+1)P_{n+1}^k(\xi_k) = (2n+1)\xi_k P_n^k(\xi_k) - nP_{n-1}^k(\xi_k) \tag{9}$$

3.2 Elastic stress–strain relation

The relations of stress-strain, according to the Hooke low for multilayer cylindrical shell with functionally graded material are defined as

$$\begin{Bmatrix} \sigma_{xx} \\ \sigma_{yy} \\ \sigma_{xy} \\ \tau_{xz} \\ \tau_{yz} \\ \tau_{zz} \end{Bmatrix}^k = \begin{bmatrix} Q_{11}^k & Q_{12}^k & 0 & 0 & 0 & Q_{13}^k \\ Q_{12}^k & Q_{22}^k & 0 & 0 & 0 & Q_{23}^k \\ 0 & 0 & Q_{66}^k & 0 & 0 & 0 \\ 0 & 0 & 0 & Q_{55}^k & 0 & 0 \\ 0 & 0 & 0 & 0 & Q_{44}^k & 0 \\ Q_{13}^k & Q_{23}^k & 0 & 0 & 0 & Q_{33}^k \end{bmatrix} \begin{Bmatrix} \varepsilon_{xx} \\ \varepsilon_{yy} \\ \gamma_{xy} \\ \gamma_{xz} \\ \gamma_{yz} \\ \varepsilon_{zz} \end{Bmatrix}^k \tag{10}$$

τ_{xy} is the shear stress, and σ_x, σ_y are the normal stress of the cylindrical shell. Q_{ij}^k are known consist of the Poisson ratio and Young modulus for the kth layer as follows

$$\begin{aligned} Q_{11}^k = Q_{22}^k = Q_{33}^k &= \frac{E^k}{1-\nu^2} \\ Q_{12}^k = Q_{13}^k = Q_{23}^k &= \frac{\nu E^k}{1-\nu^2} \\ Q_{66}^k = Q_{55}^k = Q_{44}^k &= \frac{E^k}{2(1+\nu)} \end{aligned} \tag{11}$$

where ν is the Poisson's ratio. With regard to the CUF, the vectors of strain and stress are grouped into components of the transverse and in-plane.

$$\begin{aligned} \varepsilon_p^k &= \begin{Bmatrix} \varepsilon_{xx}^k \\ \varepsilon_{\theta\theta}^k \\ \varepsilon_{x\theta}^k \end{Bmatrix}, \quad \varepsilon_n^k = \begin{Bmatrix} \varepsilon_{xz}^k \\ \varepsilon_{\theta z}^k \\ \varepsilon_{zz}^k \end{Bmatrix} \\ \sigma_p^k &= \begin{Bmatrix} \sigma_{xx}^k \\ \sigma_{\theta\theta}^k \\ \sigma_{x\theta}^k \end{Bmatrix}, \quad \sigma_n^k = \begin{Bmatrix} \sigma_{xz}^k \\ \sigma_{\theta z}^k \\ \sigma_{zz}^k \end{Bmatrix} \end{aligned} \tag{12}$$

Accordingly, the relation of constitutive for the kth layer is obtained in the following form

$$\begin{Bmatrix} \sigma_p \\ \sigma_n \end{Bmatrix}^k = \begin{bmatrix} Q_{pp}^k & Q_{pn}^k \\ Q_{np}^k & Q_{nn}^k \end{bmatrix} \begin{Bmatrix} \varepsilon_p \\ \varepsilon_n \end{Bmatrix}^k \tag{13}$$

In Eq. (13), the subscripts (n) and (p) refer to the out of plane components and in-plane, respectively. Also, $Q_{\alpha\beta}^k(\alpha, \beta = p, n)$ is the material stiffness matrix which is in the following form:

$$\begin{aligned} Q_{pp}^k &= \begin{bmatrix} Q_{11}^k & Q_{12}^k & 0 \\ Q_{12}^k & Q_{22}^k & 0 \\ 0 & 0 & Q_{66}^k \end{bmatrix}, \quad Q_{pn}^k = \begin{bmatrix} 0 & 0 & Q_{13}^k \\ 0 & 0 & Q_{23}^k \\ 0 & 0 & 0 \end{bmatrix} \\ Q_{np}^k &= \begin{bmatrix} 0 & 0 & 0 \\ 0 & 0 & 0 \\ Q_{13}^k & Q_{23}^k & 0 \end{bmatrix}, \quad Q_{nn}^k = \begin{bmatrix} Q_{55}^k & 0 & 0 \\ 0 & Q_{44}^k & 0 \\ 0 & 0 & Q_{33}^k \end{bmatrix} \end{aligned} \tag{14}$$

The relations of strain-displacement are obtained as follows

$$\varepsilon_p^k = D_p \mathrm{u}^k, \quad \varepsilon_n^k = \left(D_{np} + D_{nz}\right)\mathrm{u}^k \tag{15}$$

$\mathrm{u}^k = \{u^k, v^k, w^k\}^T$ is the field of displacement and D_{np}, D_{nz} and D_p are transverse linear and in-plane differential operator respectively and for asymmetric cases can be written in the following form

$$D_p = \begin{bmatrix} \frac{\partial}{\partial x} & 0 & 0 \\ 0 & \frac{\partial}{R\partial\theta} & \frac{1}{R} \\ \frac{\partial}{R\partial\theta} & \frac{\partial}{\partial x} & 0 \end{bmatrix}, \quad D_{np} = \begin{bmatrix} 0 & 0 & \frac{\partial}{\partial x} \\ 0 & 0 & \frac{\partial}{R\partial\theta} \\ 0 & 0 & 0 \end{bmatrix}$$
$$D_{nz} = \begin{bmatrix} \frac{\partial}{\partial z} & 0 & 0 \\ 0 & \frac{\partial}{\partial z} & 0 \\ 0 & 0 & \frac{\partial}{\partial z} \end{bmatrix} \tag{16}$$

3.3 Deployment of the CUF to multilayer FG cylindrical shell

Here, a model of variable kinematic by costs of the appropriate computational according to the CUF, is utilized to approximate the properties of the material through the thickness. The properties determination in the direction of the thickness using the Legendre Polynomials has been considered for the multilayer FG cylindrical shell. The variation of the density and stiffness matrix is created by multiplying them by a z function in the following form

$$\begin{aligned} Q(z) &= F_\gamma(z) Q_\gamma \\ \rho(z) &= F_\gamma(z) \rho_\gamma \end{aligned} \tag{17}$$

In Eq. (17), repetitious indices are summed over in the following form

$$\begin{aligned} &Q(z) = F_\gamma(z) Q_\gamma = F_0(z) Q_0 + F_r(z) Q_r + F_{N_\gamma}(z) Q_{N_\gamma} \\ &\rho(z) = F_\gamma(z) \rho_\gamma = F_0(z) \rho_0 + F_r(z) \rho_r + F_{N_\gamma}(z) \rho_{N_\gamma} \\ &r = 1, \dots, N-1 \end{aligned} \tag{18}$$

The functions of thickness in the expansion of Layer-Wise for displacements in Eq. (8), and new functions of thickness F_γ, are the same. In the present work, the expansion order is considered to $N_\gamma = 4$. Q_γ is a $[6 \times 6]$ matrix and each of the component $Q_{ij\gamma}$ can be obtained by solving the equations algebraic system which is illustrated in the following form

$$\begin{Bmatrix} Q_{ij}(z_1) \\ \vdots \\ Q_{ij}\left(z_{N_\gamma}\right) \end{Bmatrix} = \begin{bmatrix} F_0(z_1) & \cdots & F_r(z_1) & \cdots & F_{N_\gamma}(z_1) \\ \vdots & \ddots & \vdots & \ddots & \vdots \\ F_0\left(z_{N_\gamma}\right) & \cdots & F_r\left(z_{N_\gamma}\right) & \cdots & F_{N_\gamma}\left(z_{N_\gamma}\right) \end{bmatrix} \begin{Bmatrix} Q_{ij0} \\ \vdots \\ Q_{ijr} \\ \vdots \\ Q_{ijN_\gamma} \end{Bmatrix} \tag{19}$$
$$i, j = 1, \dots, 6$$

Consequently, Eq. (13) changes to the following form

$$\begin{Bmatrix} \sigma_p \\ \sigma_n \end{Bmatrix}^k = \begin{bmatrix} F_\gamma Q^k_{pp\gamma} & F_\gamma Q^k_{pn\gamma} \\ F_\gamma Q^k_{np\gamma} & F_\gamma Q^k_{nn\gamma} \end{bmatrix} \begin{Bmatrix} \varepsilon_p \\ \varepsilon_n \end{Bmatrix}^k \tag{20}$$

4. Principle of Virtual Displacements (PVDs)

The PVDs is utilized to obtain the boundary conditions and governing equations

$$\begin{aligned} &\sum_{k=1}^{N_l} \int_{A_k} \int_{z_k}^{z_{k+1}} \left[\delta\left(\varepsilon_p^k\right)^T \sigma_p^k + \delta(\varepsilon_n^k)^T \sigma_n^k \right] dA_k dz_k \\ &= \sum_{k=1}^{N_l} \delta L^k_{ine} \end{aligned} \tag{21}$$

where N_l indicates the number of layers, A_k refers to the integration domain in the $(x-\theta)$ plane, and δL_{ine} refers to the work virtual variation of the inertial loading.

By substituting the relations of strain-displacement, the field of CUF displacement and the equations of constitutive in the PVDs as follows

$$\begin{aligned} &\int_{A_k} \int_{z_k}^{z_{k+1}} \left[\left(D_p F_s \delta u_s^k\right)^T \left(F_\gamma Q^k_{pp\gamma} D_p \right.\right. \\ &\quad + F_\gamma Q^k_{pn\gamma} \left(D_{np} + D_{nz}\right) \Big) F_\gamma u_\tau^k \\ &\quad + \left(\left(D_{np} + D_{nz}\right) F_s \delta u_s^k \right)^T \\ &\quad \left(F_\gamma Q^k_{np\gamma} D_p + F_\gamma Q^k_{nn\gamma} \left(D_{np} \right.\right. \\ &\quad \left.\left. + D_{nz}\right) \Big) F_\gamma u_\tau^k \Big] dA_k dz_k \\ &= \int_{A_k} \int_{z_k}^{z_{k+1}} F_s \delta u_s^{kT} F_\gamma \rho_\gamma F_\tau \ddot{u}_\tau^k \, dA_k dz_k \end{aligned} \tag{22}$$

According to Eq. (22), the following integrals along the thickness are obtained in the following form

$$\begin{aligned} &\left(J^k_{\tau s\gamma}, J^k_{\tau_z s\gamma}, J^k_{\tau s_z\gamma}, J^k_{\tau_z s_z\gamma}\right) \\ &= \int_{z_k}^{z_{k+1}} \left(F_\tau F_s F_\gamma, \frac{\partial F_\tau}{\partial z} F_s F_\gamma, F_\tau \frac{\partial F_s}{\partial z} F_\gamma, \frac{\partial F_\tau}{\partial z} \frac{\partial F_s}{\partial z} F_\gamma \right) dz_k \end{aligned} \tag{23}$$

Considering Eq. (23), Eq. (22) is changed as follows

$$\begin{aligned} &\int_{A_k} \left\{ \left(D_p \delta u_s^k\right)^T \left(J_{\tau s\gamma} Q^k_{pp\gamma} D_p u_\tau^k + J_{\tau s\gamma} Q^k_{pn\gamma} D_{np} u_\tau^k \right.\right. \\ &\quad + J_{\tau_z s\gamma} Q^k_{pn\gamma} u_\tau^k \Big) + \left(D_p \delta u_s^k\right)^T \left(J_{\tau s\gamma} Q^k_{np\gamma} D_p u_\tau^k \right. \\ &\quad + J_{\tau s\gamma} Q^k_{nn\gamma} D_{np} u_\tau^k + J_{\tau_z s\gamma} Q^k_{nn\gamma} u_\tau^k \Big) + (\delta u_s^k)^T \\ &\quad \times \left(J_{\tau s_z\gamma} Q^k_{np\gamma} D_p u_\tau^k + J_{\tau s_z\gamma} Q^k_{nn\gamma} D_{np} u_\tau^k \right. \\ &\quad \left.\left. + J_{\tau_z s_z\gamma} Q^k_{nn\gamma} u_\tau^k \right) \right\} dA_k = \int_{A_k} \delta u_s^{kT} \rho_\gamma J^k_{\tau s\gamma} \ddot{u}_\tau^k dA_k \end{aligned} \tag{24}$$

Utilizing the theorem of Divergence to by parts integrate in 2D, yields

$$\begin{aligned} &\int_{A_k} (D_\Omega \delta u_s^k)^T u_\tau^k dA_k = -\int_{A_k} \delta u_s^{kT} (D_\Omega^T u_\tau^k) dA_k \\ &+ \oint_{\Gamma_k} \delta u_s^{kT} (I_\Omega^T u_\tau^k) d\Gamma_k \qquad \Omega = p, np \end{aligned} \tag{25}$$

In Eq. (25), Γ is the oriented outside boundary surface of A. Also, A is an area in $(x-\theta)$ plane. Matrices I_{np} and I_p are the cosine functions in the following form

$$I_p=\begin{bmatrix}\cos\left(\frac{\pi x}{L}\right) & 0 & 0\\ 0 & \frac{1}{R}\cos(\theta) & 0\\ \frac{1}{R}\cos(\theta) & \cos\left(\frac{\pi x}{L}\right) & 0\end{bmatrix}$$
$$I_{np}=\begin{bmatrix}0 & 0 & \cos\left(\frac{\pi x}{L}\right)\\ 0 & 0 & \frac{1}{R}\cos(\theta)\\ 0 & 0 & 0\end{bmatrix} \tag{26}$$

Therefore, I_{np} and I_p related to the boundary geometry are as follows

$$I_p=\begin{bmatrix}1 & 0 & 0\\ 0 & \frac{1}{R} & 0\\ \frac{1}{R} & 1 & 0\end{bmatrix},\quad I_{np}=\begin{bmatrix}0 & 0 & 1\\ 0 & 0 & \frac{1}{R}\\ 0 & 0 & 0\end{bmatrix} \tag{27}$$

Finally, the associated natural boundary conditions and governing equations are obtained in the following form

$$\int_{A_k}(\delta u_s^k)^T K^{k\tau s}u_\tau^k dA_k+\oint_{\Gamma_k}(\delta u_s^k)^T \Pi^{k\tau s}u_\tau^k d\Gamma_k = -\int_{A_k}(\delta u_s^k)^T M^{k\tau s}\ddot{u}_\tau^k dA_k \tag{28}$$

where

$$\begin{aligned}M^{k\tau s}&=I\rho_j^k J_{\tau sj}^k\\ K^{k\tau s}&=-D_p^T\left(J_{\tau sj}^k Q_{ppj}^k D_p+J_{\tau sj}^k Q_{pnj}^k D_{np}+J_{\tau s_zj}^k Q_{pnj}^k\right)\\ &\quad -D_{np}^T\left(J_{\tau sj}^k Q_{npj}^k D_p+J_{\tau sj}^k Q_{nnj}^k D_{np}+J_{\tau s_zj}^k Q_{nnj}^k\right)\\ &\quad +\left(J_{\tau_z sj}^k Q_{npj}^k D_p+J_{\tau_z sj}^k Q_{nnj}^k D_{np}+J_{\tau_z s_zj}^k Q_{nnj}^k\right)\\ \Pi^{k\tau s}&=I_p^T\left(J_{\tau sj}^k Q_{ppj}^k D_p+J_{\tau sj}^k Q_{pnj}^k D_{np}+J_{\tau s_zj}^k Q_{pnj}^k\right)\\ &\quad +I_{np}^T\left(J_{\tau sj}^k Q_{npj}^k D_p+J_{\tau sj}^k Q_{nnj}^k D_{np}+J_{\tau s_zj}^k Q_{nnj}^k\right)\end{aligned} \tag{29}$$

In Eq. (29), $K^{k\tau s}$, $\Pi^{k\tau s}$, and $M^{k\tau s}$ are the stiffness, boundary condition matrices, and nucleus of inertial, respectively, and I is the identity matrix. Also, the forms of the $K^{k\tau s}$, $\Pi^{k\tau s}$, and $M^{k\tau s}$ nucleus are as follows

$$\begin{aligned}K_{11}^{k\tau s}&=-\left(Q_{11j}\frac{\partial^2}{\partial x^2}+Q_{66j}\frac{1}{R^2}\frac{\partial^2}{\partial\theta^2}\right)J_{\tau sj}^k+Q_{55j}J_{\tau_z s_zj}^k\\ K_{12}^{k\tau s}&=-\left[\left(Q_{12j}+Q_{66j}\right)\frac{1}{R}\frac{\partial^2}{\partial x\partial\theta}\right]J_{\tau sj}^k\\ K_{13}^{k\tau s}&=-Q_{12j}\frac{1}{R}\frac{\partial}{\partial x}J_{\tau sj}^k+\left[\left(Q_{13j}+Q_{55j}\right)\frac{\partial}{\partial x}\right]J_{\tau s_zj}^k\\ K_{21}^{k\tau s}&=-\left[\left(Q_{12j}+Q_{66j}\right)\frac{1}{R}\frac{\partial^2}{\partial x\partial\theta}\right]J_{\tau sj}^k\\ K_{22}^{k\tau s}&=-\left(Q_{22j}\frac{1}{R^2}\frac{\partial^2}{\partial\theta^2}+Q_{66j}\frac{\partial^2}{\partial x^2}+\frac{Q_{44j}}{R^2}\right)J_{\tau sj}^k\\ &\quad +Q_{44j}J_{\tau s_zj}^k\end{aligned} \tag{30}$$

$$\begin{aligned}K_{23}^{k\tau s}&=-\left(Q_{22j}\frac{1}{R^2}\frac{\partial}{\partial\theta}-Q_{44j}\frac{1}{R^2}\frac{\partial}{\partial\theta}\right)J_{\tau sj}^k\\ &\quad -\left(Q_{23j}\frac{1}{R}\frac{\partial}{\partial\theta}-Q_{44j}\frac{1}{R}\frac{\partial}{\partial\theta}\right)J_{\tau s_zj}^k\\ K_{31}^{k\tau s}&=-Q_{12j}\frac{1}{R}\frac{\partial}{\partial x}J_{\tau sj}^k-Q_{55j}\frac{\partial}{\partial x}J_{\tau s_zj}^k+Q_{13j}\frac{\partial}{\partial x}J_{\tau_z sj}^k\\ K_{32}^{k\tau s}&=-\left(Q_{22j}\frac{1}{R^2}\frac{\partial}{\partial\theta}-Q_{44j}\frac{1}{R^2}\frac{\partial}{\partial\theta}\right)J_{\tau sj}^k\\ &\quad -Q_{44j}\frac{1}{R}\frac{\partial}{\partial\theta}J_{\tau s_zj}^k+Q_{23j}\frac{1}{R}\frac{\partial}{\partial\theta}J_{\tau_z sj}^k\\ K_{33}^{k\tau s}&=-\left(Q_{22j}\frac{1}{R^2}+Q_{55j}\frac{\partial^2}{\partial x^2}+Q_{44j}\frac{1}{R^2}\frac{\partial^2}{\partial\theta^2}\right)J_{\tau sj}^k\\ &\quad -\frac{Q_{23j}}{R}J_{\tau s_zj}^k+\frac{Q_{23j}}{R}J_{\tau_z sj}^k+Q_{33j}J_{\tau_z s_zj}^k\end{aligned} \tag{30}$$

$$\begin{aligned}M_{11}^{k\tau s}&=M_{22}^{k\tau s}=M_{33}^{k\tau s}=\rho_j^k J_{\tau sj}^k\\ M_{ij}^{k\tau s}&=0\qquad i\neq j\end{aligned} \tag{31}$$

Boundary condition nucleus at $x=0,L$

$$\begin{aligned}\Pi_{11}^{k\tau s}&=-\left(Q_{11j}\frac{\partial}{\partial x}+Q_{66j}\frac{1}{R^2}\frac{\partial}{\partial\theta}\right)J_{\tau sj}^k\\ \Pi_{12}^{k\tau s}&=-\left(Q_{12j}\frac{1}{R}\frac{\partial}{\partial\theta}+Q_{66j}\frac{1}{R}\frac{\partial}{\partial x}\right)J_{\tau sj}^k\\ \Pi_{13}^{k\tau s}&=-\frac{Q_{12j}}{R}J_{\tau sj}^k-Q_{13j}J_{\tau s_zj}^k\\ \Pi_{21}^{k\tau s}&=-\left(Q_{12j}\frac{1}{R}\frac{\partial}{\partial x}+Q_{66j}\frac{1}{R}\frac{\partial}{\partial\theta}\right)J_{\tau sj}^k\\ \Pi_{22}^{k\tau s}&=-\left(Q_{66j}\frac{\partial}{\partial x}+Q_{22j}\frac{1}{R^2}\frac{\partial}{\partial\theta}\right)J_{\tau sj}^k\\ \Pi_{23}^{k\tau s}&=-\frac{Q_{22j}}{R^2}J_{\tau sj}^k-\frac{Q_{23j}}{R}J_{\tau s_zj}^k\\ \Pi_{31}^{k\tau s}&=-Q_{55j}J_{\tau s_zj}^k\\ \Pi_{32}^{k\tau s}&=\frac{Q_{44j}}{R^2}J_{\tau sj}^k-\frac{Q_{44j}}{R}J_{\tau s_zj}^k\\ \Pi_{33}^{k\tau s}&=-\left(Q_{55j}\frac{\partial}{\partial x}+Q_{44j}\frac{1}{R^2}\frac{\partial}{\partial\theta}\right)J_{\tau sj}^k\end{aligned} \tag{32}$$

Consequently, Eq. (28) is simplified as:

- Governing equations

$$\begin{bmatrix}K_{11}^{k\tau s} & K_{12}^{k\tau s} & K_{13}^{k\tau s}\\ K_{21}^{k\tau s} & K_{22}^{k\tau s} & K_{23}^{k\tau s}\\ K_{31}^{k\tau s} & K_{32}^{k\tau s} & K_{33}^{k\tau s}\end{bmatrix}\begin{Bmatrix}u_\tau^k\\ v_\tau^k\\ w_\tau^k\end{Bmatrix} = -\begin{bmatrix}M_{11}^{k\tau s} & 0 & 0\\ 0 & M_{22}^{k\tau s} & 0\\ 0 & 0 & M_{33}^{k\tau s}\end{bmatrix}\begin{Bmatrix}\ddot{u}_\tau^k\\ \ddot{v}_\tau^k\\ \ddot{w}_\tau^k\end{Bmatrix} \tag{33a}$$

- Boundary conditions

$$\begin{bmatrix}\Pi_{11}^{k\tau s} & \Pi_{12}^{k\tau s} & \Pi_{13}^{k\tau s}\\ \Pi_{21}^{k\tau s} & \Pi_{22}^{k\tau s} & \Pi_{23}^{k\tau s}\\ \Pi_{31}^{k\tau s} & \Pi_{32}^{k\tau s} & \Pi_{33}^{k\tau s}\end{bmatrix}\begin{Bmatrix}u_\tau^k\\ v_\tau^k\\ w_\tau^k\end{Bmatrix}=0 \tag{33b}$$

For free vibration behavior with regard to the boundary conditions, a harmonic solution is considered as the unknown displacements in the following form (Carrera 1999)

$$\begin{Bmatrix} u_\tau^k(x,\theta,t) \\ v_\tau^k(x,\theta,t) \\ w_\tau^k(x,\theta,t) \end{Bmatrix} = \begin{Bmatrix} \sum_{m,n} u^k e^{i\omega_{mn}t} \cos\frac{m\pi x}{L} \sin n\theta \\ \sum_{m,n} v^k e^{i\omega_{mn}t} \sin\frac{m\pi x}{L} \cos n\theta \\ \sum_{m,n} w^k e^{i\omega_{mn}t} \sin\frac{m\pi x}{L} \sin n\theta \end{Bmatrix} \quad (34)$$

In Eq. (34), ω_{mn} is the natural frequency. Substituting Eq. (34) into Eq. (33a) yields an eigenvalue problem, then the eigenvalue problem solution is equal to ω_{mn}^2.

5. Discretization of the equation of transverse motion

According to boundary condition, the approximate solution for transverse linear oscillation of the sandwich cylindrical shell with an FG core can be considered as follows (Volmir 1972, Bich *et al*. 2012)

$$w_\tau^k(x,\theta,t) = \sum_{m=1}^{\bar{M}} \sum_{n=1}^{\bar{N}} W^k(t) \sin\frac{m\pi x}{L} \sin n\theta \quad (35)$$

In Eq. (35), m and n are numbers of the half and full deformation waves in the axial and circumferential directions, respectively. According to the approach which is presented in Nosi and Reddy (1991), Bhimaraddi (1999), the inertia terms related to u_τ^k and v_τ^k in Eq. (32a) is neglected, and by substituting Eq. (34) into (33a), the displacements u_τ^k and v_τ^k can be written in terms of w_τ^k.

If Eq. (32a) is denoted by Γ, the equation of motion may be found based on Galerkin's method in terms of W as follows

$$\oint \sin\frac{m\pi x}{L} \sin n\theta \, \Gamma \, d\theta dx = 0 \quad (36)$$

After substituting Eq. (35) in the third Eq. (33a), the equations of governing differential for the transverse motion of the sandwich cylindrical shell with an FG core may be obtained, after carrying out Galerkin's orthogonally integration appeared in Eq. (36).

6. Numerical results

6.1 Validation of the present work

To validation of these formulations, in Table 1, the obtained natural frequencies are compared with those presented by Pellicano (2007), Qin *et al*. (2017), and Wang *et al*. (2019). Also, in Table 2, the natural frequencies for an FG cylindrical shell at room temperature obtained from the present method are compared with those obtained by Loy *et al*. (1999) and Wang *et al*. (2018). It may easily be noted that there is a good agreement among these results.

In Fig. 4, the natural frequencies of the cylindrical shells for the various numbers of full waves are compared with experimentally results reported in Dung and Nam (2014) and Sewall and Naumann (1968). This comparison also illustrates that good agreement is obtained.

Table 1 Comparison of the natural frequencies of cylindrical shell ($L = 0.2$ m, $R = 0.1$ m, $h = 0.247 \times 10^{-3}$ m, $E = 7.12 \times 10^{10}$ N/m^2, $\rho = 2796$ kg/m^3, $\nu = 0.31$)

m	n	Present	Qin *et al*. (2017)	Pellicano (2007)	Wang *et al*. (2019c)
1	7	486.0	484.6	484.6	484.5
1	8	490.3	489.6	489.6	489.5
1	9	545.8	546.2	546.2	546.2
1	6	555.8	553.3	553.3	553.3
1	10	634.8	636.8	636.8	636.8
2	10	962.3	968.1	968.1	968.1
2	11	976.6	983.4	983.4	983.3

Table 2 Comparison of the natural frequencies of FG cylindrical shell ($L = 20$ m, $R = 1$ m, $h = 0.2 \times 10^{-3}$ m, $m = 1$, $E_m = 2.08 \times 10^{11}$ N/m^2, $E_c = 2.05 \times 10^{11}$ N/m^2, $\rho_m = 8166$ kg/m^3, $\rho_c = 8900$ kg/m^3, $\nu = 0.31$)

N	n	Present	Loy *et al*. (1999)	Wang *et al*. (2018)
0	5	11.545	11.542	11.542
0	6	16.899	16.897	16.897
0	7	23.247	23.244	23.244
0	8	30.579	30.573	30.573
1	5	11.244	11.241	11.241
1	6	16.458	16.455	16.455
1	7	22.637	22.635	22.635
1	8	29.774	29.771	29.771

In Fig. 4, the natural frequencies of the cylindrical shells for the various numbers of full waves are compared with experimentally results reported in Dung and Nam (2014)

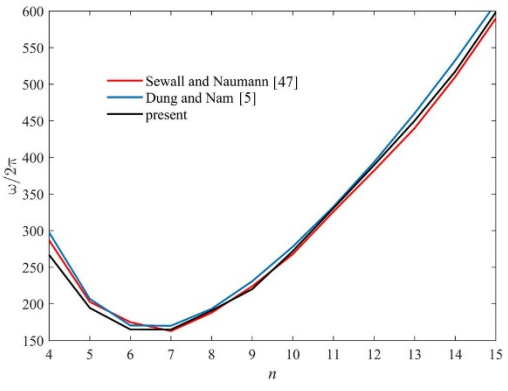

Fig. 4 Comparison of the natural frequencies of isotropic cylindrical shell ($m = 1$)

Table 3 Material properties of the constituent materials of the considered FG cylindrical shells (Duc and Thang 2015)

Material	Properties	P_0	P_{-1}	P_1	P_2	P_3
Si_3N_4 (Ceramic)	E(Pa)	3.48e11	0	-3.07e-4	2.16e-7	-8.95e-11
	ρ(Kg/m^3)	2370	0	0	0	0
SUS304 (Metal)	E(Pa)	2.01e11	0	3.08e-4	-6.53e-7	0
	ρ(Kg/m^3)	8166	0	0	0	0

Table 4 The geometric specifications of the shell

R(m)	L(m)	h_m(m)	h_u(m)	h_b(m)	m
0.5	0.75	0.0012	0.0004	0.0004	1

and Sewall and Naumann (1968). This comparison also illustrates that good agreement is obtained.

6.2 Free vibration analysis

In this section, the vibration behaviors of the sandwich cylindrical shell with an FG core based on the CUF are illustrated. The geometric characteristic and material parameters listed in Tables 3 and 4, respectively, will be utilized for the extraction of the results. Since the Poisson's ratio is assumed to be equal for ceramic and metal, thus in all solved examples, the Poisson's ratio is defined by ν, i.e., $\nu = \nu_m = \nu_c = 0.3$ also, the shell material power-law index (K) and temperature (T) are assumed to be equal to 1 and 300 K.

The effect of the circumferential and axial modes on the natural vibration responses for MFC and CFM cylindrical shells is illustrated in Figs. 5 and 6, respectively. Considering these figures, the natural frequencies for the first three axial modes are plotted. It can be deduced that increasing the axial modes leads to increasing the natural frequency. Also, the natural frequencies for various circumferential modes are presented in these figures. With regard to these figures, first, by increasing the circumferential modes, the natural frequencies are decreased to reach the critical frequency, then by increasing the circumferential modes, the natural frequencies are increased.

The various circumferential and axial modes for multilayer FG cylindrical shell may be observed in figure 7. In this figure, the first three axial modes and for each axial mode, three circumferential modes (5, 6, and 7) are investigated.

The influence of material power-law index for the FG layer of shell on the natural frequency responses of multilayer FG cylindrical shell is revealed in Table 5. It can be deduced that by increasing the material power-law index, the natural frequencies for the MFC cylindrical shell are decreased and the natural frequencies for the CFM cylindrical shell are increased. According to these results, for MFC cylindrical shell, when the percent of the ceramic properties is decreased, the natural frequencies are decreased, and for CFM cylindrical shell, when the percent of the metallic properties is decreased, the natural frequencies are increased.

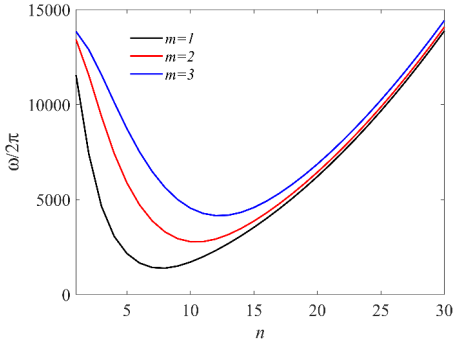

Fig. 5 The natural frequency response of the MFC cylindrical shell

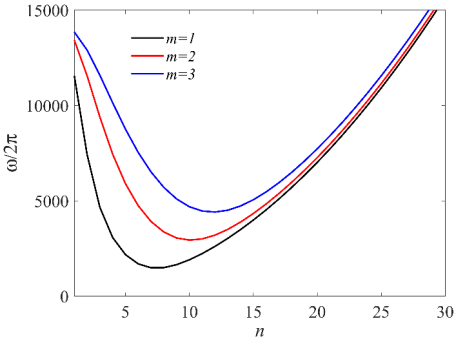

Fig. 6 The natural frequency response of the CFM cylindrical shell

Table 5 Effect of material power law index on the natural frequency responses of multilayer FG cylindrical shells ($m = 1$)

k	Case I: MFC	Case II: CFM
0.2	1614.67 (8[a])	1306.63 (7)
0.5	1492.30 (8)	1391.76 (7)
1	1390.01 (8)	1489.45 (7)
5	1222.12 (8)	1741.75 (7)
10	1185.98 (8)	1816.13 (7)

[a] The numbers in the parenthesis denote the circumferential modes (n)

Table 6 demonstrated the effect of layers thickness of shell on the natural frequency of the sandwich cylindrical shell with an FG core. With regard to this table, by

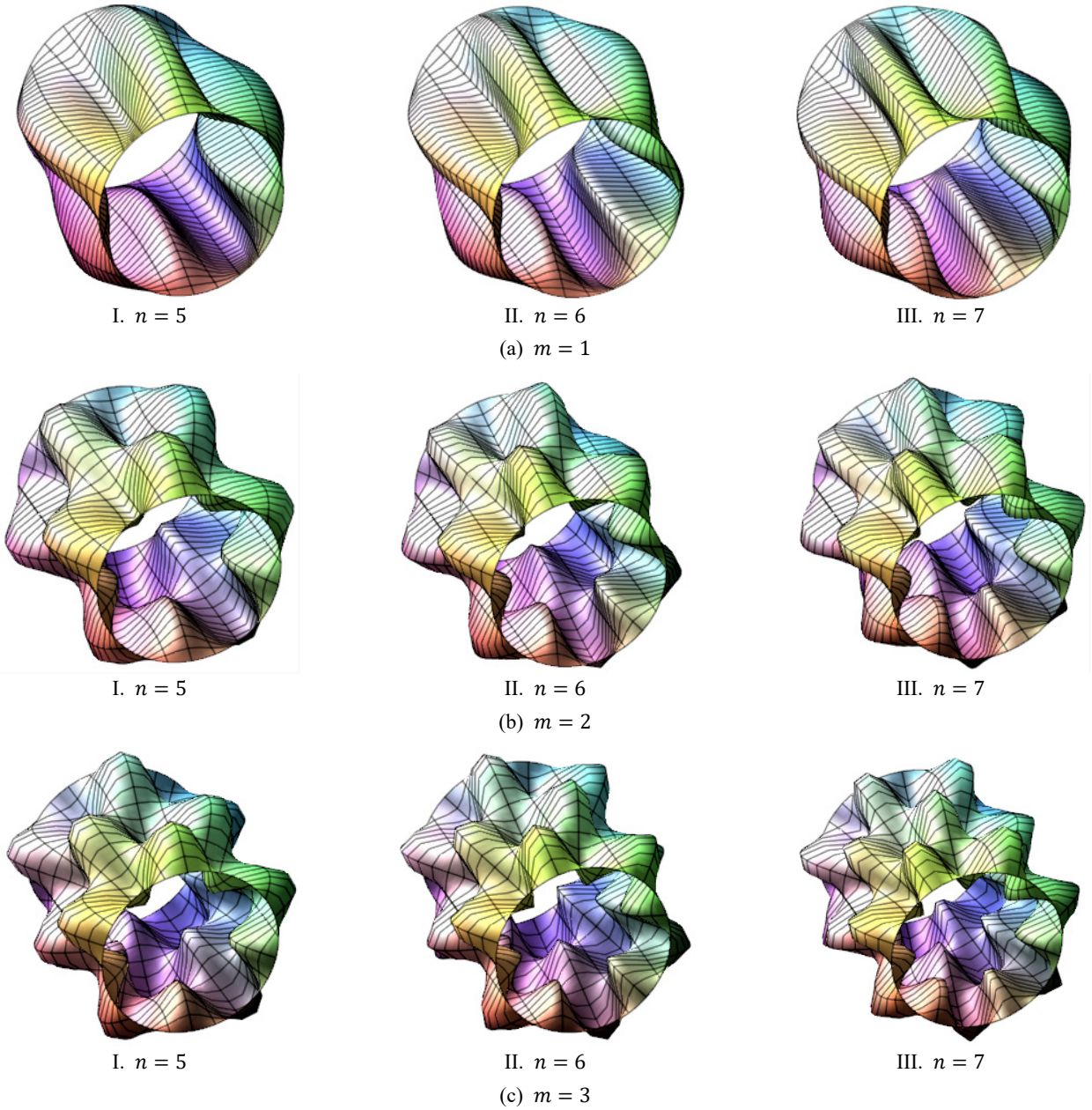

Fig. 7 The mode shapes of the sandwich cylindrical shell with an FG core

Table 6 Influence of layers thickness of shell on the natural frequency responses of the sandwich cylindrical shell with an FG core ($m = 1$)

h_u	h_m	h_b	Case I: MFC	Case II: CFM
0.0004	0.0012	0.0004	1390.01 (8[a])	1489.45 (7)
0.0008	0.0008	0.0004	1239.48 (8)	1527.18 (8)
0.0012	0.0004	0.0004	1138.18 (8)	1633.77 (8)
0.0004	0.0008	0.0008	1445.78 (8)	1391.39 (7)
0.0004	0.0004	0.0012	1528.33 (8)	1298.06 (7)

[a] The numbers in the parenthesis denote the circumferential modes (n)

Table 7 Effect of radius-to-thickness (R/h) on the natural frequency responses of the sandwich cylindrical shell with an FG core ($m = 1$)

R/h	Case I: MFC	Case II: CFM
100	2189.35 (4[a])	2346.84 (4)
150	1805.58 (5)	1901.99 (5)
200	1571.73 (7)	1659.74 (6)
250	1390.01 (8)	1489.45 (7)

[a] The numbers in the parenthesis denote the circumferential modes (n)

increasing the thickness of ceramic and metal layers, the natural frequencies of the sandwich cylindrical shell with an FG core increased and decreased, respectively.

Table 8 Effect of length-to-radius (L/R) on the natural frequency responses of the sandwich cylindrical shell with an FG core ($m = 1$)

L/R	Case I: MFC	Case II: CFM
1	2079.27 (9[a])	2205.62 (9)
1.5	1390.01 (8)	1489.45 (7)
2	1043.05 (7)	1223.26 (7)
2.5	829.94 (6)	883.99 (6)

[a] The numbers in the parenthesis denote the circumferential modes (n)

Table 9 fect of the temperature (T) on the natural frequency responses of the sandwich cylindrical shell with an FG core ($m = 1$)

T	Case I: MFC	Case II: CFM
300	1390.01 (8[a])	1489.45 (7)
350	1384.72 (8)	1482.74 (7)
400	1378.26 (8)	1475.58 (7)

[a] The numbers in the parenthesis denote the circumferential modes (n)

The influence of R/h on the natural frequencies of multilayer FG cylindrical shell may be observed in Table 7. According to this figure, by increasing the radius-to-thickness ratio, the natural frequency is decreased, whereas, the circumferential mode is increased.

The influence of length-to-radius ratio (L/R) on the natural frequencies of the sandwich cylindrical shell with an FG core is illustrated in Table 8. As shown in this Table, when the length-to-radius ratio is decreased, the natural frequency and the circumferential mode are decreased.

The influence of the various temperatures (T) on the natural frequencies of the sandwich cylindrical shell with an FG core is illustrated in Table 9. As shown in this Table, increasing the temperature leads to decreasing natural frequency.

7. Conclusions

An analytical approach was investigated to analyze the free vibration response of the sandwich cylindrical shell with an FG core according to the Carrera unified formulation (CUF). It is assumed that the FG distributions through the thickness direction. The material properties are temperature-dependent. The multilayer cylindrical shell with functionally graded material is considered with two cases: MFC and CFM. According to the PVDs, according to the CUF, the dependent boundary conditions and governing equations were obtained. The coupled governing equations are solved utilizing Galerkin's method. These results were obtained for 3D structure, because, the 3D displacement field $u(x, y, z)$ according to the CUF for the 2D plate theory, can be expanded as a set of thickness functions depending only on the thickness coordinate z and the corresponding variables depending on the in-plane coordinates x and y. In this research, we considered that the expansion order utilized for the direction of thickness is equal to 4 ($N = 4$). So, according to CUF, we could obtain the results of the free vibration analysis of 3D structure in the form of a sandwich cylindrical shell with an FG core. Some other conclusions can be summarized as follows:

- For MFC cylindrical shell, when the percent of the ceramic properties is decreased, the natural frequencies are decreased, and for CFM cylindrical shell, when the percent of the metallic properties is decreased, the natural frequencies are increased.
- By increasing the thickness of ceramic and metal layers, the natural frequencies of the sandwich cylindrical shell with an FG core increased and decreased, respectively.
- By increasing the radius-to-thickness ratio, the natural frequency is decreased, whereas, the circumferential mode is increased.
- By decreasing the length-to-radius ratio, the natural frequency and the circumferential mode are decreased.
- Increasing the axial modes leads to increasing the natural frequency.
- By increasing the circumferential modes, the natural frequencies are decreased to reach the critical frequency, and then by increasing the circumferential modes, the natural frequencies are increased.
- Increasing the temperature leads to decreasing natural frequency.

Acknowledgments

E. Carrera have been supported by the Russian Science Foundation (Grant No. 18-19-00092).

References

Ahmadi, H. and Foroutan, K. (2020), "Active vibration control of nonlinear stiffened FG cylindrical shell under periodic loads", *Smart Struct. Syst., Int. J.*, **25**(6), 643-655. http://doi.org/10.12989/sss.2020.25.6.643

Arani, A.G., Kolahchi, R. and Esmailpour, M. (2016), "Nonlinear vibration analysis of piezoelectric plates reinforced with carbon nanotubes using DQM", *Smart Struct. Syst., Int. J.*, **18**(4), 787-800. http://dx.doi.org/10.12989/sss.2016.18.4.787

Arefi, M. (2015), "The effect of different functionalities of FGM and FGPM layers on free vibration analysis of the FG circular plates integrated with piezoelectric layers", *Smart Struct. Syst., Int. J.*, **15**(5), 1345-1362. http://dx.doi.org/10.12989/sss.2015.15.5.1345

Babaei, H., Kiani, Y. and Eslami, M.R. (2019), "Large amplitude free vibrations of long FGM cylindrical panels on nonlinear elastic foundation based on physical neutral surface", *Compos. Struct.*, **220**, 888-898. https://doi.org/10.1016/j.compstruct.2019.03.064

Bhimaraddi, A. (1999), "Large amplitude vibrations of imperfect antisymmetric angle-ply laminated plates", *J. Sound Vib.*, **162**, 457-470. https://doi.org/10.1006/jsvi.1993.1133

Bich, D.H., Van Dung, D. and Nam, V.H. (2012), "Nonlinear dynamical analysis of eccentrically stiffened functionally

graded cylindrical panels", *Compos. Struct.*, **94**(8), 2465-2473. https://doi.org/10.1016/j.compstruct.2012.03.012

Bich, D.H., Dung, D.V., Nam, V.H. and Phuong, N.T. (2013), "Nonlinear static and dynamic buckling analysis of imperfect eccentrically stiffened functionally graded circular cylindrical thin shells under axial compression", *Int. J. Mech. Sci.*, **74**, 190-200. https://doi.org/10.1016/j.ijmecsci.2013.06.002

Carrera, E. (1997), "Cz requirements—models for the two dimensional analysis of multilayered structures", *Compos. Struct.*, **37**(3-4), 373-383. https://doi.org/10.1016/S0263-8223(98)80005-6

Carrera, E. (1998a), "Mixed layer-wise models for multilayered plates analysis", *Compos. Struct.*, **43**(1), 57-70. https://doi.org/10.1016/S0263-8223(98)00097-X

Carrera, E. (1998b), "Evaluation of layerwise mixed theories for laminated plates analysis", *AIAA J.*, **36**(5), 830-839. https://doi.org/10.2514/2.444

Carrera, E. (1998c), "Layer-wise mixed models for accurate vibrations analysis of multilayered plates", *J. Appl. Mech.*, **65**(4), 820-828. https://doi.org/10.1115/1.2791917

Carrera, E. (1999), "A Reissner's mixed variational theorem applied to vibration analysis of multilayered shell", *J. Appl. Mech.*, **66**(1), 69-78, https://doi.org/10.1115/1.2789171

Carrera, E. (2003), "Theories and finite elements for multilayered plates and shells: a unified compact formulation with numerical assessment and benchmarking", *Archiv. Comput. Methods Eng.*, **10**(3), 215-296. https://doi.org/10.1007/BF02736224

Carrera, E. and Demasi, L. (2002a), "Classical and advanced multilayered plate elements based upon PVD and RMVT. Part 1: derivation of finite element matrices", *Int. J. Numer. Meth. Eng.*, **55**(2), 191-231. https://doi.org/10.1002/nme.492

Carrera, E. and Demasi, L. (2002b), "Classical and advanced multilayered plate elements based upon PVD and RMVT. Part 2: numerical implementations", *Int. J. Numer. Meth. Eng.*, **55**(3), 253-291. https://doi.org/10.1002/nme.493

Carrera, E. and Ettore, A. (1995), *A Class of Two-Dimensional Theories for Anisotropic Multilayered Plates Analysis*, Accademia delle. Scienze.

Carrera, E. and Pagani, A. (2014), "Free vibration analysis of civil engineering structures by component-wise models", *J. Sound Vib.*, **333**(19), 4597-4620. https://doi.org/10.1016/j.jsv.2014.04.063

Carrera, E., Giunta, G. and Petrolo, M. (2011), *Beam Structures: Classical and Advanced Theories*, John Wiley & Sons.

Chakraborty, S., Dey, T. and Kumar, R. (2019), "Stability and vibration analysis of CNT-Reinforced functionally graded laminated composite cylindrical shell panels using semi-analytical approach", *Compos. Part B-Eng.*, **168**, 1-14. https://doi.org/10.1016/j.compositesb.2018.12.051

Cinefra, M., Carrera, E. and Valvano, S. (2015a), "Variable kinematic shell elements for the analysis of electro-mechanical problems", *Mech. Adv. Mater. Struct.*, **22**(1-2), 77-106. https://doi.org/10.1080/15376494.2014.908042

Cinefra, M., Valvano, S. and Carrera, E. (2015b), "A layer-wise MITC9 finite element for the freevibration analysis of plates with piezo-patches", *Int. J. Smart Nano Mater.*, **6**(2), 85-104. https://doi.org/10.1080/19475411.2015.1037377

Cinefra, M., Valvano, S. and Carrera, E. (2015c), "Heat conduction and thermal stress analysis of laminated composites by a variable kinematic MITC9 shell element", *Curved Layered Struct.*, **1**, 301-320. https://doi.org/10.1515/cls-2015-0017

Duc, N.D. and Thang, P.T. (2015), "Nonlinear dynamic response and vibration of shear deformable imperfect eccentrically stiffened S-FGM circular cylindrical shells surrounded on elastic foundations", *Aerosp. Sci. Technol.*, **40**, 115-127. https://doi.org/10.1016/j.ast.2014.11.005

Dung, D.V. and Nam, V.H. (2014), "Nonlinear dynamic analysis of eccentrically stiffened functionally graded circular cylindrical thin shells under external pressure and surrounded by an elastic medium", *Eur. J. Mech. A-Solid*, **46**, 42-53. https://doi.org/10.1016/j.euromechsol.2014.02.008

Foroutan, K., Shaterzadeh, A. and Ahmadi, H. (2018), "Nonlinear dynamic analysis of spiral stiffened functionally graded cylindrical shells with damping and nonlinear elastic foundation under axial compression", *Struct. Eng. Mech., Int. J.*, **66**(3), 295-303. https://doi.org/10.12989/sem.2018.66.3.295

Foroutan, K., Ahmadi, H. and Carrera, E. (2019a), "Nonlinear vibration of imperfect FG-CNTRC cylindrical panels under external pressure in the thermal environment", *Compos. Struct.*, **227**, 111310. https://doi.org/10.1016/j.compstruct.2019.111310

Foroutan, K., Shaterzadeh, A. and Ahmadi, H. (2019b), "Nonlinear dynamic analysis of spiral stiffened cylindrical shells rested on elastic foundation", *Steel Compos. Struct., Int. J.*, **32**(4), 509-519. https://doi.org/10.12989/scs.2019.32.4.509

Giunta, G., Biscani, F., Belouettar, S., Ferreira, A.J.M. and Carrera, E. (2013), "Free vibration analysis of composite beams via refined theories", *Compos. Part B-Eng.*, **44**(1), 540-552. https://doi.org/10.1016/j.compositesb.2012.03.005

Gohardani, O., Elola, M.C. and Elizetxea, C. (2014), "Potential and prospective implementation of carbon nanotubes on next generation aircraft and space vehicles: A review of current and expected applications in aerospace sciences", *Prog. Aerosp. Sci.*, **70**, 42-68. https://doi.org/10.1016/j.paerosci.2014.05.002

Lei, Z.X., Zhang, L.W., Liew, K.M. and Yu, J.L. (2014), "Dynamic stability analysis of carbon nanotube-reinforced functionally graded cylindrical panels using the element-free kp-Ritz method", *Compos. Struct.*, **113**, 328-338. https://doi.org/10.1016/j.compstruct.2014.03.035

Lei, Z.X., Zhang, L.W. and Liew, K.M. (2015a), "Elastodynamic analysis of carbon nanotube-reinforced functionally graded plates", *Int. J. Mech. Sci.*, **99**, 208-217. https://doi.org/10.1016/j.ijmecsci.2015.05.014

Lei, Z.X., Zhang, L.W. and Liew, K.M. (2015b), "Free vibration analysis of laminated FG-CNT reinforced composite rectangular plates using the kp-Ritz method", *Compos. Struct.*, **127**, 245-259. https://doi.org/10.1016/j.compstruct.2015.03.019

Lei, Z.X., Zhang, L.W. and Liew, K.M. (2016), "Analysis of laminated CNT reinforced functionally graded plates using the element-free kp-Ritz method", *Compos. Part B-Eng.*, **84**, 211-221. https://doi.org/10.1016/j.compositesb.2015.08.081

Liew, K.M. and Alibeigloo, A. (2020), "Predicting bucking and vibration behaviors of functionally graded carbon nanotube reinforced composite cylindrical panels with three-dimensional flexibilities", *Compos. Struct.*, **256**, 113039. https://doi.org/10.1016/j.compstruct.2020.113039

Liew, K.M., Pan, Z. and Zhang, L.W. (2020), "The recent progress of functionally graded CNT reinforced composites and structures", *Sci. China Phy. Mech. Astron.*, **63**(3), 234601. https://doi.org/10.1007/s11433-019-1457-2

Loy, C.T., Lam, K.Y. and Reddy, J.N. (1999), "Vibration of functionally graded cylindrical shells", *Int. J. Mech. Sci.*, **41**(3), 309-324. https://doi.org/10.1016/S0020-7403(98)00054-X

Mashat, D.S., Carrera, E., Zenkour, A.M., Al Khateeb, S.A. and Filippi, M. (2014), "Free vibration of FGM layered beams by various theories and finite elements", *Compos. Part B-Eng.*, **59**, 269-278. https://doi.org/10.1016/j.compositesb.2013.12.008

Nam, V.H., Phuong, N.T., Van Minh, K. and Hieu, P.T. (2018), "Nonlinear thermo-mechanical buckling and post-buckling of multilayer FGM cylindrical shell reinforced by spiral stiffeners surrounded by elastic foundation subjected to torsional loads", *Eur. J. Mech. A-Solid*, **72**, 393-406. https://doi.org/10.1016/j.euromechsol.2018.06.005

Neves, A.M.A., Ferreira, A.J.M., Carrera, E., Roque, C.M.C., Cinefra, M., Jorge, R.M.N. and Soares, C.M.M. (2012), "A

quasi-3D sinusoidal shear deformation theory for the static and free vibration analysis of functionally graded plates", *Compos. Part B-Eng.*, **43**(2), 711-725. https://doi.org/10.1016/j.compositesb.2011.08.009

Nosi, A. and Reddy, J.N. (1991), "A study of non-linear dynamic equations of higher-order deformation plate theories", *Int. J. Non-Linear Mech.*, **26**, 233-249. https://doi.org/10.1016/0020-7462(91)90054-W

Pagani, A., Boscolo, M., Banerjee, J.R. and Carrera, E. (2013), "Exact dynamic stiffness elements based on one-dimensional higher-order theories for free vibration analysis of solid and thin-walled structures", *J. Sound Vib.*, **332**(23), 6104-6127. https://doi.org/10.1016/j.jsv.2013.06.023

Pan, Z.Z., Zhang, L.W. and Liew, K.M. (2019), "Modeling geometrically nonlinear large deformation behaviors of matrix cracked hybrid composite deep shells containing CNTRC layers", *Comput. Meth. Appl. Mech. Eng.*, **355**, 753-778. https://doi.org/10.1016/j.cma.2019.06.041

Pellicano, F. (2007), "Vibrations of circular cylindrical shells: Theory and experiments", *J. Sound Vib.*, **303**(1-2), 154-170. https://doi.org/10.1016/j.jsv.2007.01.022

Qin, Z., Chu, F. and Zu, J. (2017), "Free vibrations of cylindrical shells with arbitrary boundary conditions: A comparison study", *Int. J. Mech. Sci.*, **133**, 91-99. https://doi.org/10.1016/j.ijmecsci.2017.08.012

Qin, Z., Pang, X., Safaei, B. and Chu, F. (2019), "Free vibration analysis of rotating functionally graded CNT reinforced composite cylindrical shells with arbitrary boundary conditions", *Compos. Struct.*, **220**, 847-860. https://doi.org/10.1016/j.compstruct.2019.04.046

Sewall, J.L. and Naumann, E.C. (1968), An experimental and analytical vibration study of thin cylindrical shells with and without longitudinal stiffeners NASA TN D-4705.

Shen, H.S. and Xiang, Y. (2012), "Nonlinear vibration of nanotube-reinforced composite cylindrical shells in thermal environments", *Comput. Methods Appl. Mech. Eng.*, **213**, 196-205. https://doi.org/10.1016/j.cma.2011.11.025

Sofiyev, A., Karaca, Z. and Zerin, Z. (2017), "Non-linear vibration of composite orthotropic cylindrical shells on the non-linear elastic foundations within the shear deformation theory", *Compos. Struct.*, **159**, 53-62. https://doi.org/10.1016/j.compstruct.2016.09.048

Song, Z.G., Zhang, L.W. and Liew, K.M. (2016), "Vibration analysis of CNT-reinforced functionally graded composite cylindrical shells in thermal environments", *Int. J. Mech. Sci.*, **115**, 339-347. https://doi.org/10.1016/j.ijmecsci.2016.06.020

Tohidi, H., Hosseini-Hashemi, S.H. and Maghsoudpour, A. (2018), "Size-dependent forced vibration response of embedded micro cylindrical shells reinforced with agglomerated CNTs using strain gradient theory", *Smart Struct. Syst., Int. J.*, **22**(5), 527-546. http://doi.org/10.12989/sss.2018.22.5.527

Viglietti, A., Zappino, E. and Carrera, E. (2019), "Analysis of variable angle tow composites structures using variable kinematic models", *Compos. Part B-Eng.*, **171**, 272-283. https://doi.org/10.1016/j.compositesb.2019.03.072

Volmir, A.S. (1972), *Non-linear Dynamics of Plates and Shells*, AS Science Edition M., USSR.

Wang, Y.Q. (2018), "Electro-mechanical vibration analysis of functionally graded piezoelectric porous plates in the translation state", *Acta Astronaut.*, **143**, 263-271. https://doi.org/10.1016/j.actaastro.2017.12.004

Wang, Y.Q. and Zhao, H.L. (2019), "Free vibration analysis of metal foam core sandwich beams on elastic foundation using Chebyshev collocation method", *Arch. Appl. Mech.*, **89**(11), 2335-2349. https://doi.org/10.1007/s00419-019-01579-0

Wang, Y.Q. and Zu, J.W. (2017a), "Nonlinear steady-state responses of longitudinally traveling functionally graded material plates in contact with liquid", *Compos. Struct.*, **164**, 130-144. https://doi.org/10.1016/j.compstruct.2016.12.053

Wang, Y.Q. and Zu, J.W. (2017b), "Porosity-dependent nonlinear forced vibration analysis of functionally graded piezoelectric smart material plates", *Smart Mater. Struct.*, **26**(10), 105014. https://doi.org/10.1088/1361-665X/aa8429

Wang, Y.Q. and Zu, J.W. (2017c), "Vibration behaviors of functionally graded rectangular plates with porosities and moving in thermal environment", *Aerosp. Sci. Technol.*, **69**, 550-562. https://doi.org/10.1016/j.ast.2017.07.023

Wang, Y., Ye, C. and Zu, J.W. (2018), "Identifying the temperature effect on the vibrations of functionally graded cylindrical shells with porosities", *Appl. Math. Mech.*, **39**(11), 1587-1604. https://doi.org/10.1007/s10483-018-2388-6

Wang, Y.Q., Wan, Y.H. and Zu, J.W. (2019a), "Nonlinear dynamic characteristics of functionally graded sandwich thin nanoshells conveying fluid incorporating surface stress influence", *Thin Wall. Struct.*, **135**, 537-547. https://doi.org/10.1016/j.tws.2018.11.023

Wang, Y.Q., Ye, C. and Zu, J.W. (2019b), "Nonlinear vibration of metal foam cylindrical shells reinforced with graphene platelets", *Aerosp. Sci. Technol.*, **85**, 359-370. https://doi.org/10.1016/j.ast.2018.12.022

Wang, Y.Q., Ye, C. and Zu, J.W. (2019c), "Vibration analysis of circular cylindrical shells made of metal foams under various boundary conditions", *Int. J. Mech. Mater. Des.*, **15**(2), 333-344. https://doi.org/10.1007/s10999-018-9415-8

Wang, Y.Q., Ye, C. and Zhu, J. (2020), "Chebyshev collocation technique for vibration analysis of sandwich cylindrical shells with metal foam core", *ZAMM J. Appl. Math. Mech.*, e201900199. https://doi.org/10.1002/zamm.201900199

Wu, C.P. and Li, H.Y. (2012), "Exact solutions of free vibration of rotating multilayered FGM cylinders", *Smart Struct. Syst., Int. J.*, **9**(2), 105-125. http://dx.doi.org/10.12989/sss.2012.9.2.105

Yang, F.L. and Wang, Y.Q. (2020), "Free and Forced Vibration of Beams Reinforced by 3D Graphene Foam", *Int. J. Appl. Mech.*, **12**(05), 2050056. https://doi.org/10.1142/S1758825120500568

Zghal, S., Frikha, A. and Dammak, F. (2018), "Free vibration analysis of carbon nanotube-reinforced functionally graded composite shell structures", *Appl. Math. Model.*, **53**, 132-155. https://doi.org/10.1016/j.apm.2017.08.021

Zhang, L.W. (2017a), "An element-free based IMLS-Ritz method for buckling analysis of nanocomposite plates of polygonal planform", *Eng. Anal. Bound. Elem.*, **77**, 10-25. https://doi.org/10.1016/j.enganabound.2017.01.004

Zhang, L.W. (2017b), "On the study of the effect of in-plane forces on the frequency parameters of CNT-reinforced composite skew plates", *Compos. Struct.*, **160**, 824-837. https://doi.org/10.1016/j.compstruct.2016.10.116

Zhang, L.W. (2017c), "Geometrically nonlinear large deformation of CNT-reinforced composite plates with internal column supports", *J. Model. Mech. Mater.*, **1**(1). https://doi.org/10.1515/jmmm-2016-0154

Zhang, L.W. and Liew, K.M. (2015), "Large deflection analysis of FG-CNT reinforced composite skew plates resting on Pasternak foundations using an element-free approach", *Compos. Struct.*, **132**, 974-983. https://doi.org/10.1016/j.compstruct.2015.07.017

Zhang, L.W. and Liew, K.M. (2016a), "Postbuckling analysis of axially compressed CNT reinforced functionally graded composite plates resting on Pasternak foundations using an element-free approach", *Compos. Struct.*, **138**, 40-51. https://doi.org/10.1016/j.compstruct.2015.11.031

Zhang, L.W. and Liew, K.M. (2016b), "Element-free geometrically nonlinear analysis of quadrilateral functionally graded material plates with internal column supports", *Compos. Struct.*, **147**, 99-110.

https://doi.org/10.1016/j.compstruct.2016.03.034
Zhang, L.W. and Selim, B.A. (2017), "Vibration analysis of CNT-reinforced thick laminated composite plates based on Reddy's higher-order shear deformation theory", *Compos. Struct.*, **160**, 689-705. https://doi.org/10.1016/j.compstruct.2016.10.102
Zhang, L.W. and Xiao, L.N. (2017), "Mechanical behavior of laminated CNT-reinforced composite skew plates subjected to dynamic loading", *Compos. Part B-Eng.*, **122**, 219-230. https://doi.org/10.1016/j.compositesb.2017.03.041
Zhang, L.W., Zhu, P. and Liew, K.M. (2014), "Thermal buckling of functionally graded plates using a local Kriging meshless method", *Compos. Struct.*, **108**, 472-492. https://doi.org/10.1016/j.compstruct.2013.09.043
Zhang, L.W., Huang, D. and Liew, K.M. (2015a), "An element-free IMLS-Ritz method for numerical solution of three-dimensional wave equations", *Comput. Meth. Appl. Mech. Eng.*, **297**, 116-139. https://doi.org/10.1016/j.cma.2015.08.018
Zhang, L.W., Li, D.M. and Liew, K.M. (2015b), "An element-free computational framework for elastodynamic problems based on the IMLS-Ritz method", *Eng. Anal. Bound. Elem.*, **54**, 39-46. https://doi.org/10.1016/j.enganabound.2015.01.007
Zhang, L.W., Lei, Z.X. and Liew, K.M. (2015c), "Buckling analysis of FG-CNT reinforced composite thick skew plates using an element-free approach", *Compos. Part B-Eng.*, **75**, 36-46. https://doi.org/10.1016/j.compositesb.2015.01.033
Zhang, L.W., Cui, W.C. and Liew, K.M. (2015d), "Vibration analysis of functionally graded carbon nanotube reinforced composite thick plates with elastically restrained edges", *Int. J. Mech. Sci.*, **103**, 9-21. https://doi.org/10.1016/j.ijmecsci.2015.08.021
Zhang, L.W., Song, Z.G. and Liew, K.M. (2015e), "State-space Levy method for vibration analysis of FG-CNT composite plates subjected to in-plane loads based on higher-order shear deformation theory", *Compos. Struct.*, **134**, 989-1003. https://doi.org/10.1016/j.compstruct.2015.08.138
Zhang, L.W., Song, Z.G. and Liew, K.M. (2015f), "Nonlinear bending analysis of FG-CNT reinforced composite thick plates resting on Pasternak foundations using the element-free IMLS-Ritz method", *Compos. Struct.*, **128**, 165-175. https://doi.org/10.1016/j.compstruct.2015.03.011
Zhang, L.W., Liew, K.M. and Reddy, J.N. (2016a), "Postbuckling analysis of bi-axially compressed laminated nanocomposite plates using the first-order shear deformation theory", *Compos. Struct.*, **152**, 418-431. https://doi.org/10.1016/j.compstruct.2016.05.040
Zhang, L.W., Liew, K.M. and Reddy, J.N. (2016b), "Postbuckling of carbon nanotube reinforced functionally graded plates with edges elastically restrained against translation and rotation under axial compression", *Comput. Meth. Appl. Mech. Eng.*, **298**, 1-28. https://doi.org/10.1016/j.cma.2015.09.016
Zhang, L.W., Liew, K.M. and Reddy, J.N. (2016c), "Postbuckling behavior of bi-axially compressed arbitrarily straight-sided quadrilateral functionally graded material plates", *Comput. Meth. Appl. Mech. Eng.*, **300**, 593-610. https://doi.org/10.1016/j.cma.2015.11.030
Zhang, L.W., Liew, K.M. and Jiang, Z. (2016d), "An element-free analysis of CNT-reinforced composite plates with column supports and elastically restrained edges under large deformation", *Compos. Part B-Eng.*, **95**, 18-28. https://doi.org/10.1016/j.compositesb.2016.03.078
Zhang, L.W., Liu, W.H. and Liew, K.M. (2016e), "Geometrically nonlinear large deformation analysis of triangular CNT-reinforced composite plates", *Int. J. Non-Linear Mech.*, **86**, 122-132. https://doi.org/10.1016/j.ijnonlinmec.2016.08.004
Zhang, L.W., Xiao, L.N., Zou, G.L. and Liew, K.M. (2016f), "Elastodynamic analysis of quadrilateral CNT-reinforced functionally graded composite plates using FSDT element-free method", *Compos. Struct.*, **148**, 144-154. https://doi.org/10.1016/j.compstruct.2016.04.006
Zhang, L.W., Song, Z.G. and Liew, K.M. (2016g), "Optimal shape control of CNT reinforced functionally graded composite plates using piezoelectric patches", *Compos. Part B-Eng.*, **85**, 140-149. https://doi.org/10.1016/j.compositesb.2015.09.044
Zhang, L.W., Zhang, Y., Zou, G.L. and Liew, K.M. (2016h), "Free vibration analysis of triangular CNT-reinforced composite plates subjected to in-plane stresses using FSDT element-free method", *Compos. Struct.*, **149**, 247-260. https://doi.org/10.1016/j.compstruct.2016.04.019
Zhang, L.W., Song, Z.G. and Liew, K.M. (2016i), "Computation of aerothermoelastic properties and active flutter control of CNT reinforced functionally graded composite panels in supersonic airflow", *Comput. Meth. Appl. Mech. Eng.*, **300**, 427-441. https://doi.org/10.1016/j.cma.2015.11.029
Zhang, L.W., Song, Z.G., Qiao, P. and Liew, K.M. (2017), "Modeling of dynamic responses of CNT-reinforced composite cylindrical shells under impact loads", *Comput. Meth. Appl. Mech. Eng.*, **313**, 889-903. https://doi.org/10.1016/j.cma.2016.10.020
Zhang, W., Liu, T., Xi, A. and Wang, Y.N. (2018), "Resonant responses and chaotic dynamics of composite laminated circular cylindrical shell with membranes", *J. Sound Vib.*, **423**, 65-99. https://doi.org/10.1016/j.jsv.2018.02.049
Zhu, P., Zhang, L.W. and Liew, K.M. (2014), "Geometrically nonlinear thermomechanical analysis of moderately thick functionally graded plates using a local Petrov–Galerkin approach with moving Kriging interpolation", *Compos. Struct.*, **107**, 298-314. https://doi.org/10.1016/j.compstruct.2013.08.001

CC